

ANALYSIS OF ECoG FEATURES FOR MOVEMENT EXECUTION USING DENOISING SOURCE SEPARATION

Aysegul Gunduz¹, Justin C. Sanchez², and Jose C. Principe¹

University of Florida

¹Computational NeuroEngineering Laboratory, Department of Electrical and Computer Engineering

²Neuroprosthetics Research Group, Department of Pediatrics, Division of Neurology
Gainesville, FL 32611

ABSTRACT

The major challenge in ECoG-based neuroprosthesis is isolating features in a spectrally and spatially broad range of sources essential for modeling motor behavior. In this study, motor-induced spectral modulations are resolved using broadband ECoG recordings passed through a filterbank of constant-Q filters. Denoising source separation is a semiblind source separation methodology which extracts hidden structures of interest within the data by exploiting prior knowledge on the observations. Herein, the methodology is utilized to extract sources that modulate within the frequency content of the hand trajectory. High signal acquisition rates (12kHz) allow for analysis of frequencies beyond the fast gamma oscillations which have been thus far discarded as background activity. Exploratory analysis suggests the first components extracted from envelopes of high spectral bands correlate with the hand trajectory and their spatial distribution covers areas of premotor and primary motor cortices.

1. INTRODUCTION

Extraction of features from neural activity that regulate motor intent and execution is the first most crucial element in building neuroprosthesis for people who have lost motor function. Brain activity produces a variety of electrical signals that can be measured via recording technologies ranging from single neuron action potentials to EEG rhythms. Collected via subdural electrodes, electrocorticography (ECoG) is spatio-temporally an intermediate level of neural activity in the spectrum of invasive to noninvasive recordings. The correlation or tuning of action potentials, isolated via microelectrode arrays that penetrate the brain tissue, to motor behavior can be easily analyzed via rate codes [1]. The challenge with ECoG, on the other hand, is to isolate sources that modulate behavior from 10^4 active neurons in cortical areas of $1\text{-}1.5\text{ cm}^2$. The human ECoG features from which continuous two-dimensional trajectories can be reconstructed are yet to be fully understood. Av-

eraged event related potentials [2, 3] and event related spectral changes (desynchronization in the mu and beta bands, synchronization in the gamma and high bands) [4, 5, 6] have been analyzed with short repetitive motor execution or imagery tasks and compared with the neural activity at rest. Online one-dimensional cursor control has been achieved by patients trained to modulate spectral amplitudes of these rhythms [7, 8]. Still, the main challenge in these systems were to not to decode kinematics, but rather to distinguish or classify between motor-evoked and rest states in neural activity.

Decoding continuous two-dimensional hand trajectories using ECoG has only been recently explored. Schalk et al. [9] computed spectral amplitudes of seven bands (8-12 Hz, 18-24 Hz, 35-42 Hz, 42-70 Hz, 70-100 Hz, 100-140 Hz, 140-190 Hz) along with the average amplitude of raw ECoG signals in 333 msec windows and linearly mapped these features to a cursor moving in a circle at 0.16 Hz via a joystick. The high dimensionality of the feature vector was reduced through a correlation-based feature selector which identifies spectral bands/channels that have high mutual information with the kinematics, while eliminating channels that have high cross-channel correlations. Sensitivity analysis showed that the important bands differed across horizontal and vertical axes of the trajectory. Pistohl et al. [10] lowpass filtered ECoG signals with 0.75 sec windows of Savitsky-Golay filters to recover cursor trajectories recorded during target selection tasks via a joystick. The smoothed signals from all channels formed the measurement vector and six kinematics at time (horizontal and vertical positions, velocities and acceleration) formed the state vector to be used in a Kalman filter. Better performance was attained with patients whose electrodes covered the motor cortex. The low frequencies, followed by the gamma band, yielded the best performance, however, the gamma band did not increase performance when combined with the low frequencies. Finally, Sanchez et al. [11] computed the power in four broad spectral bands (1-60 Hz, 60-100 Hz, 100-300 Hz, 300 Hz-6 kHz) in 100 msec windows and mapped these features to

This work was supported in part by DARPA under grant ONR-450595112, the National Science Foundation under Grant #CNS-0540304 and the Children's Miracle Network.

a cursor trajectory traced by the index fingers of patient on a computer screen. Best reconstruction was achieved in the vertical axes with the fast spectral bands and channels in the motor and premotor areas.

These experimental approaches suggests the selection of optimal ECoG feature sets in space, frequency and time requires more in depth analysis. In this study, we aim to explore spatio-temporal ECoG patterns across channels through decomposition and localization of motor-evoked features. ECoG potentials are the cumulative sum of dendritic activity and postsynaptic potentials from many synchronized sources. Within these synchronized sources, our goal is to identify the ones that modulate the motor behavior executed by the subjects. We initially perform spectral decomposition of the broadband recordings into non-overlapping bands uniformly spaced in the log warped frequency domain as means of extracting motor-induced rhythms. The feature extraction methodologies herein focus on *denoising source separation* (DSS), a recently introduced decomposition framework which extracts hidden structures of interest within data by filtering the source estimates based on accumulated knowledge, presumed signal characteristics, or experimental setups [12]. With DSS each source is extracted separately and different patterns of interest can be isolated for each source. Hence, the algorithm is computationally more efficient and exploitative compared to other source separation methods such as principal or independent component analyses [12]. We incorporate the spectral characteristics of the hand trajectories to the source separation which suggests that a slowly varying modulation in the ECoG rhythms should be sought.

2. DATA COLLECTION AND EXPERIMENTAL SETUP

The patient volunteering in this study was undergoing extra-operative subdural grid electroencephalographic monitoring for the treatment of intractable complex partial epilepsy at Shands Hospital, University of Florida¹. The patient was implanted with subdural grid electrodes which consisted of a 1.5mm thick silastic sheet embedded with 6x6 platinum-iridium electrodes (4mm diameter with 2.3mm diameter exposed surface) spaced at 1-cm center-to-center distances. The anatomical location of the grids was based upon the medical team’s recommendation for epilepsy evaluation. The approximate electrode position and numbering as indicated by the surgeon at the time of surgery is presented in Figure 1. The primary motor cortex was determined by evoked potentials and direct electrical stimulation of the subdural grids and was found to be far from the seizure focus. The 36-channel electrode grid was covering premotor (PMA),

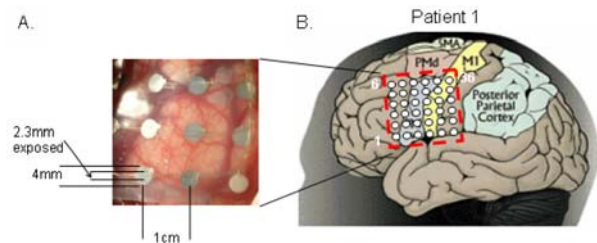


Fig. 1. A. In vivo placement of the electrode grid in a 3x3cm area of cortex and the relative electrode, gyri, sulci, and vasculature relationships. B. Electrode placement

primary motor (M1), and somatosensory (S1) cortices based on the patient’s cytoarchitecture [11]. Subdural potentials from 32 channels were recorded using a Tucker-Davis (Alachua, FL) Pentusa neural recording system at a sampling frequency of 12,207 Hz whilst the patient was engaged in the behavioral task. The recordings were collected from electrodes #1-#32 as enumerated in Figure 1. The potentials were band-pass filtered from 1Hz to 6kHz.

The behavioral tasks used in this neuroprosthetic design focus on arm reaching and pointing toward a visual input [11]. The patient was cued to continuously follow with her index finger a predefined cursor trajectory presented on an LCD screen with an active area of (20 x 30cm) while neuronal modulations from the implanted ECoG electrodes were simultaneously being recorded [11]. The trajectory consisted of a center-out task followed by a target selection task. In a single session, the patient repeated the entire task without intermission six times for each trial [11]. The behavioral trajectory recordings, originally sampled at 381.5 Hz, were downsampled to 10 Hz. The experimental task is designed to be slow enough for the patients to easily track the cursor. Figure 2 shows the power spectral densities of the horizontal and vertical trajectories computed over the entire recording session (4 mins).

3. SPECTRAL DECOMPOSITION

The rhythmicity of mesoscopic and macroscopic signals provides a means of quantitatively describing the recordings. The correlations between rhythms and actions, events or stimuli can be measured through the modulations of the rhythms. Throughout the history of EEG technology, EEG frequencies have been conveniently classified into bands [13]. ECoG allows for higher spectral resolution than EEG and fast gamma bands have shown synchronization with a variety of visual, auditory, motor and imagery tasks [14]. This motivates us to study the possibilities of capturing neural ensemble activities with ECoG synchronizing at even higher frequencies. Recent work has been published on the ultra-

¹The experimental paradigms were approved by the University of Florida Institutional Review Boards.

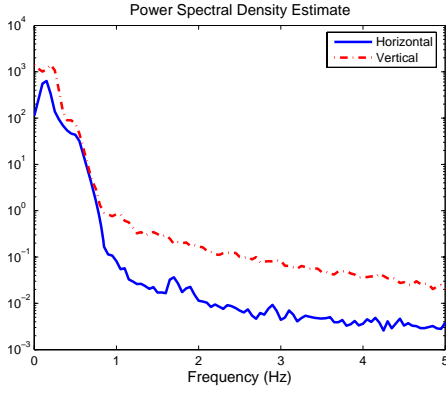


Fig. 2. Power spectral density of the horizontal and vertical hand trajectories during the experimental session.

fast frequencies and full-band EEG, claiming that the range of EEG is much broader than it has been assumed [15], which suggests an even broader spectral range for ECoG. Since our signal acquisition systems is capable of sampling at 12,207 Hz, we opt to analyze all frequency ranges upto 6 kHz (Nyquist frequency). These very high frequencies have mainly been discarded as background activity or noise [16] and never have been incorporated in neuroprosthesis technologies.

We decompose the broadband spectrum into non-overlapping intervals of equal bandwidth in the logarithmic frequency domain through a bank of *constant-Q filters*. The parameter Q is defined as the quality of a signal and is related to the ratio of the center frequency to the bandwidth of the bandpass filter. Constant Q -filters refer to a family of filters for which this ratio is held constant. For lower center frequencies the spectral band is narrow, whereas the passband around high center frequencies are wider. We start out with a large number of filters in case the bands require further merging or splitting throughout the analysis. The logarithmic spectral range from $f_1 = 8$ Hz to $f_{n+1} = 6$ kHz is uniformly divided into $n = 32$ segments with cut-off frequencies:

$$f_k = \exp(\ln(f_{n+1}/f_1)/n) f_{k-1}, \quad k = 2, \dots, n \quad (1)$$

which yields a central frequency to bandwidth ratio of $f_c/B = 4.85$ for each $[f_{k-1}, f_k]$ band. The very narrow bandwidth allocated to slow potentials suggest that for the Q -filter design the number of filters need not be higher than $n = 32$. For each of the frequency bands, we designed linear-phase FIR filters and compensated for the group-delay.

4. DENOISING SOURCE SEPARATION

Linear source separation methodologies can be applied to the filtered datasets to explore any causal relationship be-

tween the decomposed sources and the motor behavior. Any source separation algorithm based on the linear mixing assumption of hidden sources is formulated as:

$$\begin{aligned} \mathbf{X} &= \mathbf{AS} + \nu, \\ \hat{\mathbf{S}} &= \mathbf{WX}, \end{aligned} \quad (2)$$

where the observation matrix, \mathbf{X} , consists of M measurements recorded over the observation time $t = 1, \dots, T$. These measurements are assumed to be linear combinations of N sources, denoted by the source matrix \mathbf{S} , collected under Gaussian noise, ν . If the measurements are collected through spatial sensors, the mixing matrix \mathbf{A} yields the spatial patterns of the sources [12]. The demixing matrix \mathbf{W} yields the source estimates, $\hat{\mathbf{S}}$.

Unlike blind source separation methodologies, DSS exploits prior knowledge about the sources to extract desired structures within the data (e.g. non-Gaussianity, spectral content, general shape patterns etc.) [12]. This is achieved by iteratively filtering the current source estimates through *denoising functions* chosen to emphasize and maximize the desired properties in current source estimates. Each source is extracted separately (one component at a time) and thus different patterns of interest can be isolated for each source.

The DSS algorithm consists of four successive steps [17]:

1. Centering and whitening the data through eigenvalue decomposition.

$$\mathbf{Y} = \mathbf{D}^{-1/2} \mathbf{VX} \quad (3)$$

where \mathbf{D} is the diagonal matrix of eigenvalues of the covariance matrix of \mathbf{X} , and the matrix \mathbf{V} is made up of the corresponding eigenvectors. The whitening transform makes the covariance structure of the data uniform (i.e. $\mathbf{YY}^T = \mathbf{I}$) and any orthogonal projection in the whitened space yields uncorrelated components [17]. Thereby, the advantage of whitening is that an orthogonal demixing matrix, \mathbf{W} , would decompose the whitened data, \mathbf{Y} , into uncorrelated sources, $\hat{\mathbf{S}}$.

2. Source estimation by demixing the data:

$$\hat{\mathbf{s}}_i = \mathbf{w}_i^T \mathbf{X}, \quad (4)$$

where \mathbf{w}_i is a column of the demixing matrix. This linear projection of whitened data also yields sources with unit covariance.

3. Denoising the source estimates:

$$\mathbf{s}_i^+ = \mathbf{f}(\hat{\mathbf{s}}_i) \quad (5)$$

$\mathbf{f}(\cdot)$ is the denoising function which is chosen to maximize the desired properties on the source estimate. Denoising functions can be linear or nonlinear to utilize the prior information on the data.

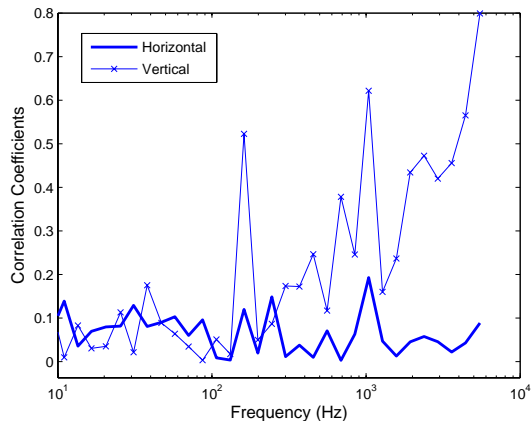


Fig. 3. Correlation coefficients between the first extracted components from the 32 spectral bands and the hand trajectory.

4. Reestimation and orthogonalization of the demixing matrix:

$$\mathbf{w}_i = \mathbf{X}\mathbf{s}_i^{+T} \quad (6)$$

The reestimated demixing vector is orthogonalized to the previously found columns of \mathbf{W} through Gram-Schmidt orthogonalization [17] in order to yield uncorrelated source estimates in the next iteration.

Steps 2-4 are iterated for each source estimate until the angle between the previous and current demixing estimates is less than a threshold ($\epsilon=0.1^\circ$). The whole process is repeated for as many components and denoising functions as necessary limited only by the number of observed variables. In the case of linear denoising, the algorithm is equal to the power-method implementation of principal component analysis (PCA) applied to the covariance matrix of the denoised signal [12]. The components in this case are ranked by the prominence of the desired characteristics (rather than the amount of variance they explain)[17].

In Figure 2, we observe that the most prominent oscillations for the target tracking task are below 1 Hz and thus choose to perform denoising based on frequency content in this band. The denoising function employed in this analysis is a low-pass filter with a cutoff frequency at 1 Hz. Hence in the source separation, we are seeking neural rhythmic sources which exhibit amplitude modulations in this band.

5. RESULTS

The modulation of the rhythms can be captured by the envelopes of bandpass filtered signals. The upper envelopes are extracted by interpolating the local maxima of the rhythms. Denoising source separation is applied to the downsampled

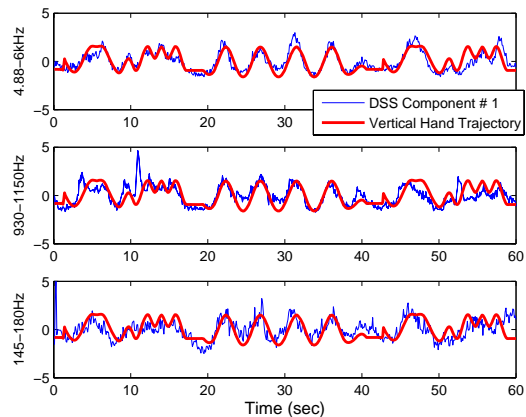


Fig. 4. Highly correlated components extracted from three spectral bands superimposed on the vertical hand trajectory. The components and the trajectory have been normalized to unit variance.

envelopes from each spectral band to extract only the first components which show the most prominent desired characteristics². The correlation coefficients between the first extracted components in each of the 32 spectral bands and the hand trajectory dimensions are plotted in Figure 3 as a function of the central frequency of the spectral bands. Several frequency bands show high modulation with the vertical hand position centered around 160 Hz, 1 kHz and 5 kHz. The extracted components (denoised sources) in these frequency bands are superimposed on the vertical hand positions in Figure 4. The components and the trajectories in the figure are normalized to unit variance. The components in each band alone are able to track the trajectories throughout the target selection task (timesteps in Figure 4: 20-40 secs), whereas the center-out task would have a better reconstruction as a combination of the bands (timesteps in Figure 4: 5-20 secs and 40-60 secs).

The mixing vectors of the denoised sources in Figure 4 are superimposed on the electrode grid in Figure 5. The contour plots are the interpolations of the spatial mixing coefficients that make up the first column³ of the mixing matrix \mathbf{A} in Eqn (2). These contour maps indicate the contributions of the extracted components in the recordings. For instance, a high mixing coefficient over an electrode in Figure 5 indicates that the source is an important component of the signal recorded from that electrode. In Figure 5, we observe that the contributions of the highly correlated sources extracted in high frequency bands are spread across most of the electrode grid, suggesting that a large cortical area, in-

²The desired characteristics fade out in the following components.

³The first column corresponds to the first extracted source which shows the most prominent desired characteristics.

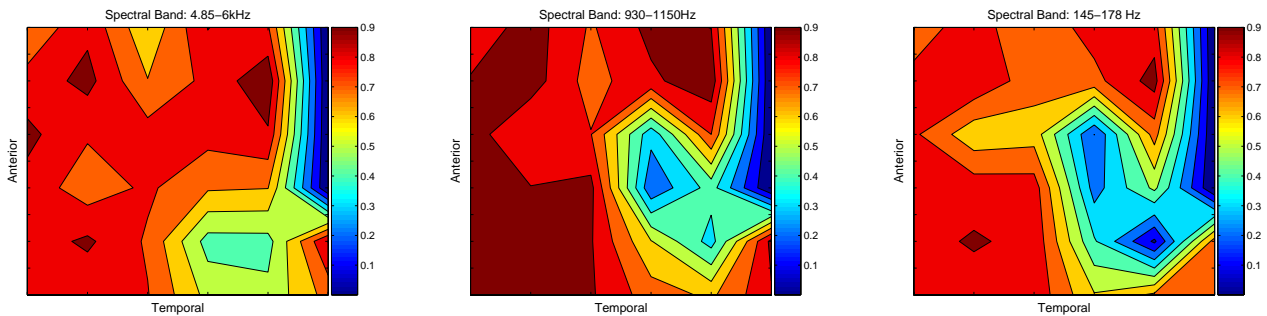


Fig. 5. Mixing vectors of the extracted components in Figure 4 are spatially superimposed over the subdural electrodes. The color coded coefficients indicate the contributions of the denoised sources over the electrode recordings.

cluding Brodmann areas 4 and 6, is synchronized at very fast frequencies. This result is not intuitive as high frequencies synchronize more locally and propagate smaller distances [14]. It is possible that the high correlations are due to the sinusoid-like nature of the desired trajectory, i.e., the results may be overfits. Characterization of overfitted results is possible through surrogate datasets which have the same Fourier amplitudes (power spectra) as the data but have random phases [18]. Surrogates generated this way mimic the autocorrelation function of the original time series, but any other structure in the data is lost. Figure 6 depicts the first DSS components extracted by creating one surrogate for each channel of the raw recordings and filtering them in the same spectral bands. The correlation coefficients between the vertical trajectories have significantly reduced to $\{0.06, 0.07, 0.15\}$. This surrogate analysis weakens the possibility of overfitted results with the original recordings.

6. DISCUSSION

With denoising source separation we were able to extract components from the channels that were highly correlated with the hand trajectories. This was achieved by spectrally inspecting the desired trajectories and denoising the source estimates based on frequency content. The results suggest that a spectral and spatial subset of channels can be selected to model the hand trajectories. The correlation coefficients between the trajectories and the denoised sources extracted from the constant-Q filterbank outputs hint at which frequency bands should be selected. From Figure 3 it is obvious that for the vertical hand position the bands with central frequencies of 160 Hz, 1 kHz and 5 kHz can be selected for modeling the trajectories with high reconstruction performance. The number of model parameters for these bands can be further decreased by selecting channels that have high mixing coefficients across the three bands (as indicated in Figure 5).

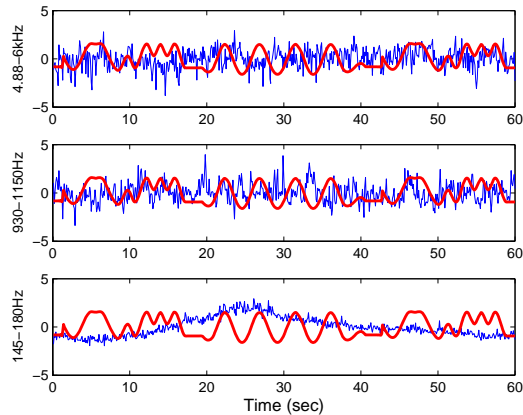


Fig. 6. Components extracted from surrogate data in the same spectral bands as Figure 4 are superimposed on the vertical hand trajectory.

In the results, we have mostly focused on the features modulating the vertical hand trajectory as the correlations of the extracted components with the horizontal hand trajectories are much lower (recall Figure 3). This may be related to the lower spatial span in this axis (i.e. low deviation of activity from the origin), as well as the vertical orientation of the experimental screen or the electrode coverage of the motor cortex (low tuning for the horizontal directions). Nevertheless, this exploratory analysis indicates feasibility of cursor control using amplitude modulations from a broad spectrum of ECoG frequency bands.

7. REFERENCES

- [1] A. P. Georgopoulos, J. F. Kalaska, R. Caminiti and J. T. Massey “On the relations between the direction of two-dimensional arm movements and cell discharge in primate

- motor cortex,” *Journal of Neuroscience*, vol. 2, no. 11, pp. 1527-1537, November 1982.
- [2] S. P. Levine, J. E. Huggins, S. L. BeMent, R. K. Ramesh, L. A. Schuh, E. A. Paasaro, M. M. Rohde, and D. A. Ross, “Identification of electrocorticogram patterns as the basis for a direct brain interface,” *American Clinical Neurophysiology Society*, vol. 16, no. 5, pg. 439, September 1999.
- [3] J. E. Huggins, S. P. Levine, S. L. BeMent, R. K. Ramesh, L. A. Schuh, E. A. Paasaro, M. M. Rohde, D. A. Ross, K. V. Elisevich, and B. J. Smith, “Detection of event-related potentials for development of a direct brain interface,” *American Clinical Neurophysiology Society*, vol. 16, no. 5, pg. 448, September 1999.
- [4] N. E. Crone, D. L. Miglioretti, B. Gordon, J. M. Sieracki, M. T. Wilson, S. Uematsu, and R.P. Lesser, “Functional mapping of human sensorimotor cortex with electrocorticographic spectral analysis: I. Alpha and beta event-related desynchronization,” *Brain*, vl. 121, pp. 2271-2299, 1998.
- [5] N. E. Crone, D. L. Miglioretti, B. Gordon, and R.P. Lesser, “Functional mapping of human sensorimotor cortex with electrocorticographic spectral analysis: II. Event-related synchronization in the gamma band,” *Brain*, vl. 121, pp. 2301-2315, 1998.
- [6] G. Pfurtscheller, B. Graimann, J. E. Huggins, S. P. Levine, and L.A. Schuh, “Spatiotemporal patterns of beta desynchronization and gamma synchronization in corticographic data during self-paced movement,” *Clinical Neurophysiology*, vol. 114, pp. 1226-1236, 2003.
- [7] E. C. Leuthardt, G. Schalk, J. R. Wolpaw, D. M. Moran, and J. G. Ojemann, “A brain-computer interface using electrocorticographic signals in humans,” *Journal of Neural Engineering*, vol. 1, pp. 63-71, 2004.
- [8] E. A. Felton, J. A. Wilson, J. C. Williams, and P. C. Garell, “Electrocorticographically controlled brain-computer interfaces using motor and sensory imagery in patients with temporary subdural electrode implants,” *Journal of Neurosurgery*, vol. 106 pp. 495-500, March 2007.
- [9] G. Schalk, J. Kubanek, K. J. Miller, N. R. Andersen, E.C. Leuthardt, J. G. Ojemann, D. Limbrick, D. Moran, L. A. Gerhardt, and J. R. Wolpaw, “Decoding two-dimensional movement trajectories using electrocorticographic signals in humans,” *Journal of Neural Engineering*, vol. 4, pp. 264-275, 2007.
- [10] T. Pistohl, T. Ball, A. Schulze-Bonhage, A. Aertsen, and C. Mehring, “Prediction of arm movement trajectories from ECoG-recordings in humans,” *Journal of Neuroscience Methods*, vol. 167, pp. 105-114, 2008.
- [11] J. C. Sanchez, A. Gunduz, J. C. Principe and P. R. Carney, “Extraction and Localization of Mesoscopic Motor Control Signals for Human ECoG Neuroprosthetics,” *submitted to Journal of Neuroscience Methods*, vol. 167, pp. 63-81, 2008.
- [12] J. Sarela and H. Valpola, “Denoising Source Separation”, *Journal of Machine Learning Research*, vol.6 , pp. 233-272, 2005.
- [13] R. Cooper, J. W. Osselton, and J. C. Shaw, *EEG Technology*, Butterworth & Co. Publishers, London, 1969.
- [14] K. J. Miller, E. C. Leuthardt, G. Schalk, R. P. N. Rao, N. R. Anderson, D. M. Moran, J. W. Miller and J. G. Ojemann, “Spectral changes in cortical surface potentials during motor movement,” *Journal of Neuroscience*, vol. 27, no. 9 , pp. 2424-2432, February 2007.
- [15] E. Niedermeyer, *Guest Editor, Special Issue: Ultrafast Frequencies and Full-Band EEG*, *Journal of Clinical EEG & Neuroscience*, October 2005.
- [16] W. J. Freeman, “Origin, structure, and role of background EEG activity. Part 1. Analytic Amplitude,” *Clinical Neurophysiology*, vol. 115, pp. 2077-2088, 2004.
- [17] A. Ilin, H. Valpola and E. Oja, “Explatory analysis of climate data using source separation methods”, *Neural Networks*, vol. 19, pp. 155-167, 2006.
- [18] T. Schreiber, and A. Schmitz, “Surrogate Time Series”, *Physica D*, vol. 142, pp. 346-382, 2000.